Available online at www.sciencedirect.com
ScienceDirect
Earth and Planetary Science Letters 256 (2007) 81–89
EPSL
www.elsevier.com/locate/epsl

Nonlinear thermoremanence acquisition and implications for paleointensity data

Peter A. Selkin [a,b,*], Jeffrey S. Gee [a], Lisa Tauxe [a]

[a] *Scripps Institution of Oceanography, University of California, San Diego, La Jolla, CA 92093, USA*
[b] *San Diego City College, 1313 Park Boulevard, San Diego, CA 92101, USA*

Received 16 August 2006; received in revised form 9 January 2007; accepted 9 January 2007
Available online 19 January 2007
Editor: M.L. Delaney

Abstract

In paleointensity studies, thermoremanence is generally regarded as a linear function of ambient magnetic field at low fields comparable to that of the present-day Earth. We find pronounced nonlinearity at low fields for a class of materials with silicate-hosted magnetite that otherwise perform well in paleointensity experiments. We model this nonlinearity with narrow size ranges of large, acicular single domain grains, which are most likely in a vortex state (i.e. nonuniformly magnetized, sometimes labeled pseudosingle domain). Simple TRM theory predicts that even certain single domain particles will also exhibit a nonlinear response, saturating in fields as low as the Earth's. Such behavior, although likely to be rare, may bias some paleointensity estimates. The bias is especially pronounced when the laboratory field is higher than the ancient field. Fortunately, the fundamental assumption that thermoremanence is proportional to applied field can (and should) be routinely checked at the end of successful paleointensity experiments by adding two extra heating steps.

Keywords: paleointensity; Thellier experiment; thermoremanent magnetization; silicate-hosted magnetite

1. Assumptions of paleointensity experiments

Estimates of the intensity of Earth's magnetic field in the past – absolute paleointensities – are essential for understanding the behavior and past history of the geodynamo. Paleointensity measurements have been used to argue for models of the timing of inner core growth [1–3], to investigate the processes controlling magnetic reversals and superchrons [4–8], and to investigate dynamo activity on other planetary bodies [9]. Paleointensity measurements are also increasingly considered in analyses of paleosecular variation, the history of change in the geometry of the geomagnetic field [10]. Typical absolute paleointensity estimates are the same order of magnitude as the present Earth's field (~30–60 μT), though lower and higher estimates do exist in the literature and have been significant in understanding geodynamo behavior (e.g. [1,3,11]).

Though useful, absolute paleointensity measurements are difficult to obtain. In essence, absolute paleointensity

* Corresponding author. Current address: Interdisciplinary Arts and Sciences, University of Washington Tacoma, Box 358436, 1900 Commerce Street, Tacoma, WA 98402-3100, USA. Fax: +1 253 692 5718.

E-mail address: paselkin@u.washington.edu (P.A. Selkin).

0012-821X/$ - see front matter © 2007 Elsevier B.V. All rights reserved.
doi:10.1016/j.epsl.2007.01.017

estimates are based on determining the ratio between a specimen's thermoremanent magnetization (TRM; See Table 1) and the field in which the rock acquired that TRM [12,13]. The history and magnetic properties of many rocks render them useless for absolute paleointensity experiments. Igneous rocks, baked sediments, heated archaeological samples (e.g. fired clay) and in some cases high-temperature metamorphic rocks are, generally speaking, the only materials that acquire a TRM, and are therefore the only candidates for absolute paleointensity experiments. The growth of magnetic particles after the rock acquires a primary TRM [14], a secondary heating episode due to burial or intrusion [15], the presence of coarse (multidomain) magnetic particles [16], and a variety of other geological factors can affect a rock's usefulness in absolute paleointensity studies, making "good" paleointensity specimens a rare and precious commodity. Recent paleointensity studies have indicated that rocks containing nanometer-scale magnetite inclusions in silicate minerals tend to avoid problems associated with secondary grain growth and multidomain effects, and therefore can yield reliable paleointensity estimates [1,17].

Paleointensity experiments themselves are fraught with difficulty. The confounding effects of changes in a rock's capacity to carry a TRM, magnetic anisotropy due to the preferred orientation of elongate magnetic particles, and differences between laboratory and natural cooling rates, among other problems, are discussed at length elsewhere (see e.g. [17–19]). Here we focus on a fundamental assumption of paleointensity experiments: that rocks acquire a TRM (both in the laboratory and in nature) in direct proportion to the field in which the remanence is acquired. For most geological materials and for geomagnetic fields with intensities comparable to the present Earth's, this assumption is reasonable. However, for some combinations of materials and field conditions, this linear relationship breaks down. Indeed, the basic theory of single domain ferromagnetism [20] predicts that all ferromagnetic materials will saturate at high fields. In this study we illustrate a distinctly nonlinear relationship between TRM and applied field, where deviations from linearity occur at fields that are geologically reasonable (as low as 20 μT). We show that this nonlinear relationship between TRM and the applied

Table 1
Terms, symbols, and abbreviations used in this paper

Term (abbreviation or symbol)	Definition
Blocking temperature (T_b)	The temperature below which the magnetization of a particle is stable (i.e. independent of applied magnetic field) over geologically relevant time scales.
Curie temperature (T_c)	The temperature at which a ferromagnetic material becomes paramagnetic and loses its ability to retain a remanent magnetization (due to the loss of exchange coupling between atoms).
Isothermal remanent magnetization (IRM)	Magnetization acquired by an assemblage of magnetic particles briefly exposed to an intense magnetic field (typically at room temperature).
Paleointensity estimate (B_{est})	Estimate of the intensity of the Earth's magnetic field at one particular sampling location and one particular episode in geologic history.
Pseudosingle domain grain	A ferromagnetic particle that has saturation remanence and stability similar to but somewhat lower than those of single domain particles. Some pseudosingle domain particles may be nonuniformly magnetized (i.e. some of their atomic magnetic moments are out of alignment with those of the rest of the particle, for example in a vortex configuration), but are not divided into separate magnetic domains.
Remanence anisotropy	The difference among remanent magnetizations acquired in fields of different orientations relative to a rock sample.
Remanent magnetization or remanence	Magnetization remaining in the absence of an applied magnetic field.
Saturation isothermal remanent magnetization or saturation remanence (SIRM, M_{rs})	Maximum (isothermal) remanent magnetization acquired by a material exposed to strong magnetic fields.
Saturation magnetization (M_s)	Maximum magnetization (not remanent magnetization) acquired by a material exposed to strong magnetic fields.
Single domain grain	A ferromagnetic particle (e.g. magnetite) that is small enough to be uniformly magnetized and behaves, essentially, as a single magnetic dipole. Materials with single domain grains are generally regarded as the most stable recorders of geomagnetic field variations. These materials are characterized by high saturation remanence relative to saturation magnetization, and by remanence that is not changed by exposure to relatively strong magnetic fields (i.e. high coercivity).
Thermoremanent magnetization (TRM, M_{trm})	Magnetization acquired by an assemblage of magnetic particles as they cool through their range of blocking temperatures.
Vortex state	A nonuniform state of magnetization in which some of the atomic magnetic moments of a particle are arranged in a curled pattern.

field can in some cases cause significant bias in absolute paleointensity estimates. We present a simple test to assess and, in many cases, mitigate this bias. Although we focus here on absolute paleointensity determinations from the Thellier double heating method [12], the bias introduced by nonlinearity will also affect paleointensities determined by other methods e.g. [13], and our test applies to all absolute paleointensity methods (including microwave, e.g. [21,22]).

In a typical absolute paleointensity experiment, a specimen is given a TRM (M_{trm}) in a known lab field (B_{lab}) in an effort to mimic the original remanence (natural remanent magnetization or NRM, M_{nrm}) acquired in nature. In a Thellier double heating experiment [12,23], the NRM is demagnetized and a partial TRM is imparted in a series of steps carried out at progressively higher temperatures, thus allowing the isolation of particular components in a multi-component NRM or the identification of a temperature range over which the specimen's capacity to acquire TRM does not alter. In the case of a generalized absolute paleointensity experiment, the ancient field estimate (B_{est}) is:

$$B_{\mathrm{est}} = \frac{M_{\mathrm{nrm}}}{M_{\mathrm{trm}}} B_{\mathrm{lab}}.$$

In the Thellier technique, the NRM/TRM ratio is determined for each step. Ideally, the lab field should be chosen to equal the ancient field. In the trivial case where the two match precisely, then linearity between applied field and magnetization is not required to estimate the paleofield. However, in practice, when heating a large number of specimens (all of which may have experienced different ancient fields) it is impractical to match the ancient fields precisely. Typically, lab fields are chosen arbitrarily (usually in the range 10–80 μT) and so the resulting paleofield estimates in general require that TRM be a linear function of the applied field.

In the process of Thellier-type experiments on specimens from the Stillwater layered intrusion (Selkin et al., in prep.), comparison of paleointensity results from sister samples using two lab fields (15 and 25 μT) yielded statistically distinct mean values (Wilcoxon ranked-sum test [24]; $p = 0.0003828$; mean paleointensities, corrected for cooling rate and anisotropy, of 39.0 ± 11.2 and 42.3 ± 11.8 μT, respectively), with higher mean values associated with higher lab fields. The laboratory fields used in the experiment were chosen as a compromise between trying to match the ancient field value and the presumed benefit of low fields in facilitating identification of multidomain effects [25].

Additional experiments (600 °C TRM as function of applied field, Fig. 1A) showed a pronounced nonlinear relationship between M_{trm} and B_{lab}, with deviations from linearity occurring at applied fields at the low end of the range of present day field.

2. Materials

Rocks used in the present study were collected in the Middle and Upper Banded Series of the Stillwater Complex, a large (~180 km^2 exposed), ultramafic to anorthositic intrusion at the edge of the Wyoming Craton in Montana, USA [26]. Specimen pp043b4 is a minicore, gabbroic in composition, from an exposure of Olivine Bearing Zone III (Middle Banded Series) on Picket Pin Mountain. Specimens smc9903i6 and smc9916e3 are from cores drilled by the Stillwater Mining Company during the construction of their East Boulder adit. Both are anorthositic in composition: smc9903i6 is from anorthosite layer AN-II, and smc9916e3 is from Gabbronorite III (Upper Banded Series).

The characteristics of smc9916e3 are in many respects similar to those of anorthosite M428, which was used in a previous paleointensity study [17]. However, none of the rocks used in this study have the high $M_{\mathrm{rs}}/M_{\mathrm{s}}$ ratios characteristic of purely elongate single domain particles noticed by [17]. For example, hysteresis measurements on chips from site pp043 (measured on a Princeton Measurements MicroMag alternating gradient force magnetometer) yielded $M_{\mathrm{rs}}/M_{\mathrm{s}}$ ratios of approximately 0.1 and B_{c} values of 9.2 mT. These values are consistent with a vortex remanence state, often called pseudosingle domain (PSD) in the literature [27].

3. Methods

All Stillwater specimens were heated in air to 600 °C, and cooled in fields of 15, 20, 30, 40, and 50 μT to impart a TRM. A 30 μT step was repeated after the aforementioned steps to evaluate the effect of alteration. A final 75 μT step was then carried out. Because the Stillwater specimens often exhibit substantial remanence anisotropy [17,28], we also evaluated the dependence of the specimens' TRM on orientation in the laboratory field by carrying out pairs of heating cycles with the specimens in different orientations. In addition, we carried out pairs of heating steps with the samples rearranged in the oven to test whether cooling rate (which varies as function of position in the oven) could account for the nonlinearity of TRM acquisition. Specimens were also given IRMs in a field of 2.0 T as a basis for normalization. Similar experiments, carried out on basaltic glass specimens, are described in online Supplement A.

4. Results

Specimens from the Stillwater Complex acquired an increasingly intense TRM in fields of increasing intensity, though the relationship between the applied field and the TRM acquired is not always linear (especially sm9916e3 in Fig. 1A). On the other hand, glass specimens acquired a TRM in proportion to the applied field (online Supplement A; all glass data were fit by lines with correlation coefficients $R > 0.99$).

One possible explanation for the nonlinear acquisition of TRM seen in Fig. 1A is simply that the specimens' TRM capacity changes during the repeated heating steps. For the Stillwater specimens, minimal changes in some specimens' ability to acquire a TRM were observed. Repeated TRM acquisition in the same field yielded similar results for most specimens (e.g., steps 2 and 9 for pp043b4 in a 30 μT field in Fig. 1A are identical). Furthermore, rearranging specimens to test for anisotropy and cooling rate did not result in significant changes in TRM.

5. Néel single domain theory of TRM

Standard Néel theory for TRM in non-interacting single domain particles [20] provides an adequate explanation for the observed field dependence. The TRM data are well fit by a hyperbolic tangent function, the functional form of $M_{\mathrm{trm}}(B_{\mathrm{lab}})$ as predicted by Néel's theory [29]:

$$M_{\mathrm{trm}}(B_{\mathrm{lab}}) = M_{\mathrm{rs}}\tanh[VM_{\mathrm{s}}(T_{\mathrm{B}})B_{\mathrm{lab}}/kT_{\mathrm{b}}]$$

where M_{rs} is saturation remanence, V is grain volume, T_{B} is blocking temperature, $M_{\mathrm{s}}(T_{\mathrm{B}})$ is saturation magnetization at the blocking temperature, and k is Boltzmann's constant. We thus fit our TRM data to a function of the form:

$$M_{\mathrm{trm}}(B_{\mathrm{lab}}) = \alpha\tanh[\beta B_{\mathrm{lab}}].$$

Néel theory predicts that specimens will become saturated with respect to TRM in some field (the intensity of which is inversely related to β). According to the Néel equation, TRM is a strong function of blocking temperature, which is defined as the temperature at which a given particle with magnetic energy

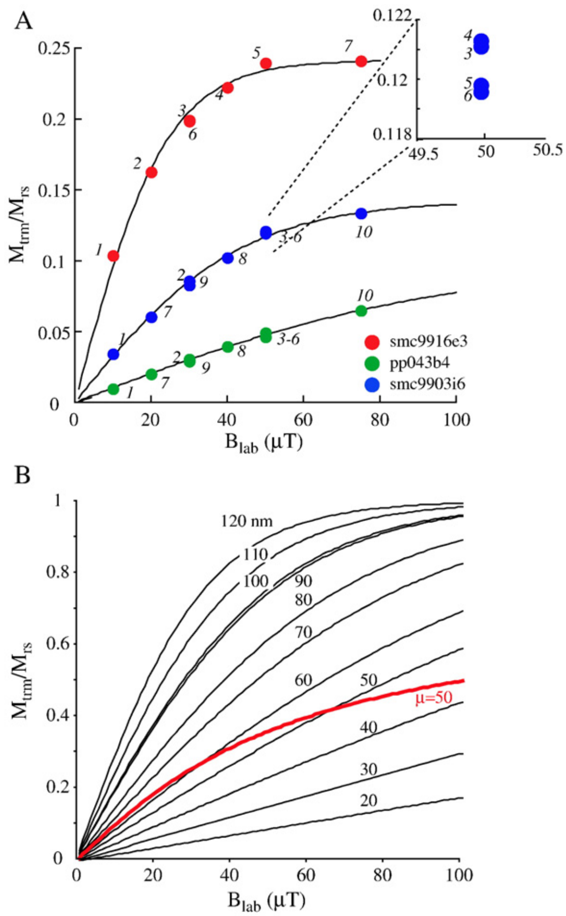

Fig. 1. Nonlinear dependence of thermoremanent magnetization (M_{trm}) on applied field from Stillwater specimens and model particles. A: TRM of representative Stillwater Complex rocks acquired in laboratory fields (B_{lab}) of 15, 20, 30, 40, 50, and 75 μT, and hyperbolic tangent fit to data ($f(x) = \alpha\tanh(\beta x)$). Applied field in TRM experiments was along z (downcore) coordinate axis; TRM used here is component parallel to z axis. Data and curve fits are normalized to saturation IRM acquired in a field of 2 T along the z axis. Saturation TRM is most likely lower than saturation IRM due to the preferred orientation of elongate magnetite particles in silicates. The order of TRM acquisition steps is shown for each specimen (italic numbers). For some specimens (e.g. pp043b4), multiple TRM acquisition steps were carried out at the same temperature to identify effects of alteration, cooling rate, and sample orientation in the laboratory field. The 30 μT step was repeated (steps 2 and 9) to evaluate the effect of alteration. Steps 5 and 6 were carried out with specimen positions rearranged in laboratory oven (relative to steps 3 and 4) to assess cooling rate effect; in steps 4 and 5, specimen orientations were varied (relative to steps 3 and 6) to assess effect of anisotropy. B: Thermoremanent magnetization acquired by a randomly-oriented population of elongate magnetite particles (a:b:c of 10:1:1) during cooling in geologically-reasonable applied magnetic fields. Red line: TRM acquisition for a gaussian distribution of grain sizes ($\mu = 50$ nm; $\sigma = 50$ nm).

density $K(T_b)$ is superparamagnetic, i.e. has a relaxation time of order hundred seconds. The magnetic energy density is a function of shape:

$$\frac{1}{2}\Delta N \mu_0 M_s(T_b)^2$$

where $\Delta N = \frac{1}{3}\left[1-\frac{2}{5}\left(2-\frac{b}{a}-\frac{c}{a}\right)\right]$, a, b, and c are the axial dimensions of an ellipsoidal particle and μ_0 is the permeability of free space. In the modeling exercises discussed here, we use the empirical relationship of Moskowitz [30] of $\frac{M_s(T_b)}{M_s(T_0)} = \left(\frac{T_c - T_b}{T_c}\right)^\gamma$ where T_c is the Curie temperature and γ is ~0.43 for magnetite. The low TRM saturation fields require that grain sizes are large (~100 nm along c, the smallest dimension). The TRM acquisition curves are less linear when the grains are acicular (Fig. 1B shows expected curves for a range of grain widths, all with aspect ratio of a:b:c::10:1:1). Although Néel single domain theory may provide an imperfect description of the TRM acquisition of actual specimens [29], the extent to which our Stillwater data are fit by the hyperbolic tangent function (Fig. 1A) and the similarity between TRM acquisition data and models (Fig. 1B) suggest that Néel theory is at least a reasonable approximation for our purposes.

Although the model curves in Fig. 1B are for populations of identical size particles, the Stillwater specimens' narrow range of unblocking temperatures (90% between 560–580 °C; [31]) suggests a narrow grain size distribution. Such a distribution of fine acicular magnetite is not unexpected in these and other mafic intrusive rocks. Selkin et al. [17] describe rocks with a remanence anisotropy of a factor of 2.5 (τ_{max}/τ_{min}) and infer acicular grains (corroborated by observations by Xu et al. [32]). Similar inferences based on rock–magnetic data have been published for other mafic and anorthositic plutons [33,34]. Direct observations of silicate-hosted magnetite indicate that crystallographically controlled magnetite is common in plagioclase and pyroxene in slowly cooled mafic intrusions [35–38]. We believe that the nonlinear relationship between TRM and applied field will cause similar effects in rock types with magnetic carriers like those in the Stillwater.

6. Bias in paleointensity experiments due to nonlinear TRM acquisition

For specimens with such a nonlinear relationship between TRM and weak applied field, absolute paleointensity estimates will be biased (Fig. 2). The sense of this bias depends on the relationship between the lab field and ancient field. If the lab field is lower than the ancient field, then the paleointensity experiment underestimates the ancient field (Fig. 2A). Under the typical assumption of linearity, the ratio of the original NRM (M_{nrm}) to TRM acquired in the laboratory field (M_{trm}) is proportional to the ratio between the estimated ancient field (B_{est}) and the lab field (B_{lab}), such that on a graph of M against B, the corresponding sets of points (B_{lab}, M_{trm}) and (B_{est}, M_{nrm}) should be colinear. However, if TRM is a nonlinear function of applied field (e.g. $M \propto \tanh(B)$), and specimens become saturated with respect to TRM in weak applied fields, M_{nrm} actually corresponds to a higher ancient field (B_{anc}) than expected under the assumption of linearity. Alternatively, if the laboratory applied field is higher than the ancient field, then the ancient field will be overestimated (Fig. 2B). In both cases, the magnitude of the paleointensity bias depends on the size/shape of the particles as well as on the ratio of the laboratory and ancient fields.

Fig. 3 illustrates the bias for two particular simulated cases: Fig. 3A shows the effect for a simulated population of elongate particles (10:1:1), and Fig. 3B shows the effect for a simulated population of nearly equant (1.5:1:1) particles. In both cases, grain shape was assumed to be the cause of anisotropy. Both simulations assume an ancient field intensity of 50 μT; the bias is calculated as $[(B_{est} - B_{anc})/B_{anc}] \times 100$, corresponding to the percentage difference between the vertical lines labeled B_{est} and B_{anc} in Fig. 2. These figures illustrate four salient points. First, bias depends on shape, such that elongate particles show a much larger bias than nearly equant particles do. Second, for a given aspect ratio, larger single-domain particles show a larger bias. Third, the greater the difference between B_{anc} and B_{lab}, the greater the bias in the paleointensity estimate. For example, for an ancient field of 50 μT and 100 nm acicular (10:1:1) particles, a lab field of 20 μT yields an estimate of 38.4 μT and a lab field of 40 μT gives 45.2 μT. The fourth (and least significant) is an asymmetry in the bias (for a given $|B_{lab} - B_{anc}|$) such that if the lab field is higher than the ancient field, the bias is larger. A higher laboratory applied field tends to produce more of a bias than does a lower laboratory field. For the same example given above, lab fields of 60 and 80 μT yield ancient field estimates of 55.5 and 68.3 μT, respectively. These overestimates (11%, 36%) are larger than the corresponding underestimates (10%, 23%) for the same absolute differences between laboratory and ancient fields.

The rocks from the Stillwater layered intrusion, with a narrow size distribution of elongate ferromagnetic particles, are unusual, but are by no means unique. In many cases, such particles have been sought after as reliable carriers of very ancient magnetizations [17,33,36,39]. It is

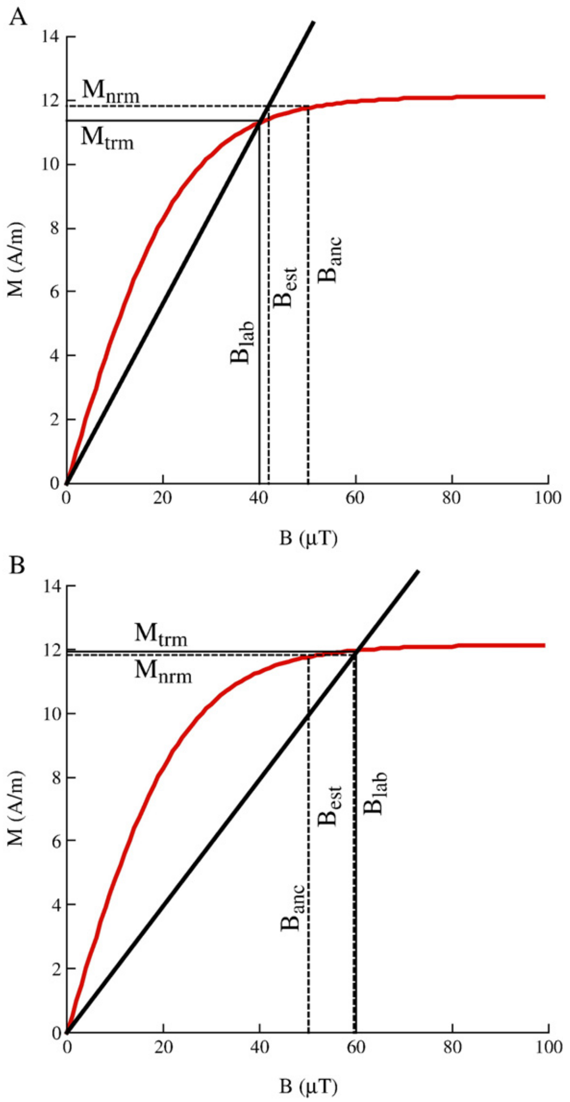

Fig. 2. Schematic representations of effects of nonlinear TRM acquisition on simulated paleointensity experiments for different laboratory field intensities. In both cases, ancient field B_{anc}=50.0 μT. Red curves: TRM acquisition of rock specimen (hyperbolic tangent fit to smc9916e3 data). Bold black lines: fundamental assumption of paleointensity experiments (i.e. $M_{nrm}/M_{trm}=B_{anc}/B_{lab}$). A: Laboratory field ($B_{lab}$, 40.0 μT)<ancient field (B_{anc}). M_{trm}=11.3 A/m; M_{nrm}=11.8 A/m. Paleointensity estimated in experiment, B_{est}=41.8 μT. The paleointensity experiment thus underestimates the ancient field by 8 μT (16% of B_{anc}). B: B_{lab}, 60.0 μT>B_{anc}. M_{trm}=12.0 A/m; M_{nrm}=11.8 A/m; B_{est}=59.0 μT. The paleointensity experiment thus overestimates the ancient field by 9 μT (18% of B_{anc}).

also possible that fine intergrowths (e.g. oxyexsolution in titanomagnetite, interlayered hemoilmenite as documented by [40]) might have correspondingly narrow grain size distributions and somewhat elongate particles. Even without a narrow distribution of grain sizes, nonlinear behavior may still significantly affect paleointensity estimates (on order of 10%): broader grain size distributions are probably more common in most geologic materials, but even with a range of grain sizes (e.g. the normal distribution used in Fig. 1B. with μ=50 nm and σ=50 nm), the presence of large, elongate grains is expected to result in a nonlinear relationship between TRM and applied field (Fig. 1B). For nearly equant grains (1.5:1:1), a bias of several percent is possible depending on the ancient field, laboratory applied field, and grain size.

7. Addition of a nonlinearity check to paleointensity experiments

To assess the degree to which a paleointensity experiment has been affected by nonlinear TRM acquisition, we recommend the simple addition of a

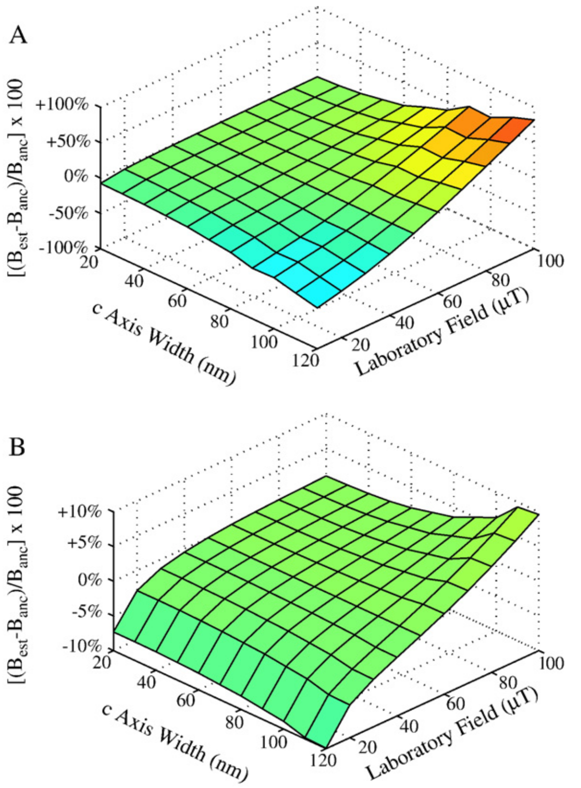

Fig. 3. Percent difference between paleointensity estimated in simulated Thellier experiments (B_{est}) and true ancient field (B_{anc}) for a range of particle sizes and laboratory field values. In all cases, B_{anc}=50 μT. Positive values on the vertical axis (warm colors) indicate an overestimate of the ancient field by the Thellier technique; negative values (darker cool colors) indicate an underestimate. A: Elongate particles with a 10:1:1 aspect ratio (a:b:c axis). Particles with c<about 20 nm are superparamagnetic (T_{ub}<25 °C). B: Nearly equant particles (a:b:c::1.5:1:1). Note different vertical scale.

field dependence check to Thellier experiments. Such a check could be carried out during the course of paleointensity experiments (as are pTRM checks) or at the end of successful experiments if the samples have not altered appreciably during laboratory heating. In the nonlinearity check, specimens should be given a TRM in two laboratory fields besides the field used in the Thellier experiment. We suggest choosing laboratory fields that bracket the range of the specimens' estimated paleointensities. The additional heating steps required in the nonlinearity check may cause samples' capacity to acquire a TRM to change, so we suggest that an additional pTRM check or similar quality assurance be carried out after or during the nonlinearity check. A diagram illustrating the check is included in online Supplement B. This nonlinearity check is similar to, but much simpler than, the method of Wilson [41]. A hyperbolic tangent function, fit to the TRM data, can then be used to estimate the degree to which the estimated ancient fields are biased by nonlinear TRM acquisition (following Fig. 2). A more appropriate ancient field estimate can be calculated using the hyperbolic tangent function, or data from specimens that are affected by nonlinear TRM acquisition to a large degree can be discarded. The NRM of such specimens may not accurately record the ancient field in which they acquired their remanence, and consequently might bias paleointensity distributions and adversely affect compilations of paleointensity data. Python source code to analyze data from a nonlinearity check is included in online Supplement C. The software provided outputs a paleointensity estimate based on the full TRM dataset as well as error bounds based on a jackknife procedure (see [42]).

As an example, TRM acquisition and paleointensity data are provided in online Supplement C for the three Stillwater specimens. Thellier experiments were carried out in laboratory applied fields of 25 μT on specimen pp043b4, and 15 μT on specimens smc9903i6 and smc9916e3. Specimen pp034b4 yielded a paleointensity of 18.0 μT (not corrected for the effects of anisotropy and cooling rate; Selkin et al., in press). Applying the nonlinear TRM correction does not change the paleointensity estimate appreciably (the corrected value is 17.8 μT). In the case of specimen smc9903i6, the Thellier experiment yielded a paleointensity value of 34.8 μT. Corrected for the effects of nonlinear TRM acquisition, however, the estimated paleointensity value is 44.4 μT (jackknife uncertainty estimates $+0.3/-0.1$ μT). Specimen smc9916e3 is nearly saturated with respect to TRM in fields approximately equal to the estimated ancient field of 27.8 μT. No nonlinear TRM correction can be applied: the paleointensity estimate for smc9916e3 is therefore a lower bound on the actual geomagnetic field intensity.

8. Conclusions and suggestions for future studies

Although absolute paleointensity studies are based on the proportionality between a rock's thermoremanent magnetization and the field in which the rock was magnetized, this relationship does not hold for all rock types at all field intensities. This may lead to a bias in paleointensity estimates. The magnitude and sense of the bias is a function of the size and shape of the remanence-carrying phases in the rock and the intensity of the laboratory and ancient fields in which the rock acquired its TRM.

Rocks containing elongate magnetic particles are particularly susceptible to the problem of nonlinear TRM acquisition. Such particles are often characterized as pseudosingle domain (PSD), nonuniformly magnetized, or vortex state [27] and are common in intrusive igneous and metamorphic rocks (e.g. [36,39,43–45]). In contrast, submarine basaltic glass, in which the remanence is most likely carried by very fine particles close to the transition between superparamagnetic and single-domain states [46–49], is notably free from the problem of nonlinear TRM acquisition associated with intrusive rocks (see online Supplement A).

Segments of the absolute paleointensity record – particularly the Archean – that rely heavily on data from intrusive rocks or from mineral separates from intrusive rocks should be viewed with skepticism until the bias is assessed on a study-by-study basis. Several studies of Archean intrusive rocks have attributed the rocks' remanence to "pseudosingle domain" [11,50,51] or "elongate" [17,52] magnetite particles. Furthermore, there has been recent interest in stable remanent magnetizations recorded by fine, lamellar intergrowths of hemoilmenite [40]: such intergrowths may also be susceptible to the problems illustrated here. This is not to imply that the magnetic carriers in Archean intrusive rocks are different from those formed at other times, but rather that the paleomagnetic record from the Archean relies heavily on such rocks [53]. We suggest that care be taken to characterize the magnetic carriers in all igneous and metamorphic rocks used in paleointensity experiments beyond merely identifying them as pseudosingle domain on a Day et al. plot [54]. The precautions described in this paper should be taken if there is the chance that the specimens contain elongate and/or nonuniformly magnetized magnetic particles.

Acknowledgments

We are grateful to the Stillwater Mining Company for allowing us to sample their archived drill cores, and to Julie Bowles for providing specimens from her basaltic glass study. Jason Steindorf did most of the laboratory measurement for this study. We thank Andrew Biggin, editor Peggy Delaney, and one anonymous reviewer for insightful comments that substantially broadened the applicability of this paper. This study was funded by NSF grants EAR9902895 and EAR0087551.

Appendix A. Supplementary data

Supplementary data associated with this article can be found, in the online version, at doi:10.1016/j.epsl.2007.01.017.

References

[1] J.A. Tarduno, R.D. Cottrell, A.V. Smirnov, The paleomagnetism of single silicate crystals: recording geomagnetic field strength during mixed polarity intervals, superchrons, and inner core growth, Rev. Geophys. 44 (2006) RG1002, doi:10.1029/2005RG000189.
[2] B.A. Buffett, The thermal state of Earth's core, Science 299 (2003) 1675–1676.
[3] C.J. Hale, Paleomagnetic data suggest link between the Archean–Proterozoic boundary and inner-core nucleation, Nature 329 (1987) 233–237.
[4] L. Tauxe, Long-term trends in paleointensity: the contribution of DSDP/ODP submarine basaltic glass collections, Phys. Earth Planet. Int. 156 (2006) 223–241.
[5] A.J. Biggin, D.N. Thomas, Analysis of long-term variations in the geomagnetic poloidal field intensity and evaluation of their relationship with global geodynamics, Geophys. J. Int. 152 (2003) 392–415 (2).
[6] P.A. Selkin, L. Tauxe, Long term variations in palaeointensity, Philos. Trans. R. Soc. Lond. 358 (2000) 1065–1088.
[7] M. Perrin, M. Prévot, E.A. Mankinen, Low intensity of the geomagnetic field in Early Jurassic time, J. Geophys. Res. 96 (1991) 14197–14210.
[8] M. Prévot, E.A. Mankinen, R.S. Coe, C.S. Grommé, The Steens Mountain (Oregon) geomagnetic polarity transition 2. Field intensity variations and discussion of reversal models, J. Geophys. Res. 90 (1985) 10417–10448.
[9] S.M. Cisowski, D.W. Collinson, S.K. Runcorn, A. Stephenson, M. Fuller, A review of lunar paleointensity data and implications for the origin of lunar magnetism, J. Geophys. Res. 88 (1983) A691–A704 (Suppl.).
[10] J.J. Love, C.G. Constable, Gaussian statistics for palaeomagnetic vectors, Geophys. J. Int. 152 (2003) 515–565.
[11] M. Macouin, J.P. Valet, J. Besse, K. Buchan, R. Ernst, M. LeGoff, U. Scharer, Low paleointensities recorded in 1 to 2.4 Ga Proterozoic dykes, Superior Province, Canada, Earth Planet. Sci. Lett. 213 (2003) 79–95.
[12] E. Thellier, O. Thellier, Sur l'intensité du champ magnétique terrestre dans le passé historique et géologique, Ann. Geophys. 15 (1959) 285–378.
[13] J. Shaw, A new method of determining the magnitude of the paleomagnetic field: application to five historic lavas and five archaeological samples, Geophys. J. R. Astron. Soc. 39 (1974) 133–141.
[14] A.V. Smirnov, J.A. Tarduno, Thermochemical remanent magnetization in Precambrian rocks: are we sure the geomagnetic field was weak? J. Geophys. Res. 110 (2005) B06103, doi:10.1029/2004JB003445.
[15] Y. Yu, D.J. Dunlop, Multivectorial paleointensity determination from the Cordova Gabbro, southern Ontario, Earth Planet. Sci. Lett. 203 (2002) 983–998.
[16] S. Levi, The effect of magnetite particle size on paleointensity determinations of the geomagnetic field, Phys. Earth Planet. Int. 13 (1977) 245–259.
[17] P.A. Selkin, J.S. Gee, L. Tauxe, W.P. Meurer, A.J. Newell, The effect of remanence anisotropy on paleointensity estimates: a case study from the Archean Stillwater Complex, Earth Planet. Sci. Lett. 183 (2000) 403–416.
[18] A.V. Smirnov, J.A. Tarduno, Magnetic hysteresis monitoring of Cretaceous submarine basaltic glass during Thellier paleointensity experiments: evidence for alteration and attendant low field bias, Earth Planet. Sci. Lett. 206 (2003) 571–585.
[19] J. Bowles, J.S. Gee, D.V. Kent, E. Bergmanis, J. Sinton, Cooling rate effects on paleointensity estimates in submarine basaltic glass and implications for dating young flows, Geochem. Geophys. Geosyst. 6 (2005) Q07002, doi:10.1029/2004GC000900.
[20] L. Néel, Théorie du trainage magnétique des ferro magnétiques en grains fins avec applications aux terres cuites, Ann. Geophys. 5 (1949) 99–137.
[21] D.N. Thomas, M.J. Hill, A.S. Garcia, Comparison of the Coe–Thellier–Thellier and microwave palaeointensity techniques using high-titanium titanomagnetites: results from a Tertiary basaltic intrusion from the Sydney Basin, New South Wales, Earth Planet. Sci. Lett. 229 (2004) 15–29.
[22] D. Walton, S. Snape, T.C. Rolph, J. Shaw, J. Share, Application of ferrimagnetic resonance heating to palaeointensity determinations, Phys. Earth Planet. Int. 94 (1996) 183–186.
[23] R.S. Coe, The determination of paleointensities of the Earth's magnetic field with emphasis on mechanisms which could cause non-ideal behavior in Thellier's method, J. Geomag. Geoelectr. 19 (1967) 157–178.
[24] J.A. Rice, Mathematical Statistics and Data Analysis, Duxbury Press, Belmont, CA, 1995.
[25] Y. Yu, L. Tauxe, A. Genevey, Toward an optimal geomagnetic field intensity determination technique, Geochem. Geophys. Geosyst. 5 (2004) Q02H07, doi:10.1029/2003GC000630.
[26] I.S. McCallum, The Stillwater Complex, in: R.G. Cawthorn (Ed.), Layered Intrusions, Developments in Petrology, vol. 15, Elsevier, Amsterdam, 1996, pp. 441–484.
[27] L. Tauxe, H.N. Bertram, C. Seberino, Physical interpretation of hysteresis loops: micromagnetic modeling of fine particle magnetite, Geochem. Geophys. Geosyst. 3 (2002) 10 1055, doi:10.1029/2001GC000241.
[28] J.S. Gee, W.P. Meurer, P.A. Selkin, M.J. Cheadle, Quantifying three-dimensional silicate fabrics in cumulates using cumulative distribution functions, J. Petrol. 45 (2004) 1983–2009.
[29] D.J. Dunlop, K.S. Argyle, Thermoremanence, anhysteretic remanence, and susceptibility of submicron magnetites: nonlinear field dependence and variation with grain size, J. Geophys. Res. 102 (1997) 20199–20210.

[30] B. Moskowitz, Methods for estimating Curie temperatures of titanomaghemites from experimental Js–T data, Earth Planet. Sci. Lett. 53 (1981) 84–88.
[31] P. A. Selkin, Archean Paleointensity from Layered Intrusions, Ph.D. Thesis, University of California, San Diego, 2003.
[32] W. Xu, J.W. Geissman, R. van der Voo, D.R. Peacor, Electron microscopy of iron oxides and implications for the origin of magnetizations and rock magnetic properties of Banded Series rocks of the Stillwater Complex, Montana, J. Geophys. Res. 102 (1997) 12139–12157.
[33] M.E. Evans, M.W. McElhinny, A.C. Gifford, Single domain magnetite and high coercivities in a gabbroic intrusion, Earth Planet. Sci. Lett. 4 (1968) 142–146.
[34] G.S. Murthy, M.E. Evans, D.I. Gough, Evidence of single-domain magnetite in the Michikamau Anorthosite, Can. J. Earth Sci. 8 (1971) 361–370.
[35] J.M. Feinberg, G.R. Scott, P.R. Renne, H.R. Wenk, Exsolved magnetite inclusions in silicates: features determining their remanence behavior, Geology 33 (2005) 513–516.
[36] P.R. Renne, G.R. Scott, J.M.G. Glen, J.M. Feinberg, Oriented inclusions of magnetite in clinopyroxene: source of stable remanent magnetization in gabbros of the Messum Complex, Namibia, Geochem. Geophys. Geosyst. 3 (2002) 10, doi:10.1029/2002GC000319 (1079).
[37] P.O. Sobolev, Orientation of acicular iron–ore mineral inclusions in plagioclase, Int. Geol. Rev. 32 (1990) 616–628.
[38] C. Frandsen, S.L.S. Stipp, S.A. McEnroe, M.B. Madsen, J.M. Knudsen, Magnetic domain structures and stray fields of individual elongated magnetite grains revealed by magnetic force microscopy (MFM), Phys. Earth Planet. Int. 141 (2004) 121–129.
[39] S.S. Harlan, L.W. Snee, J.W. Geissman, A.J. Brearley, Paleomagnetism of the Middle Proterozoic Laramie anorthosite complex and Sherman Granite, southern Laramie Range, Wyoming and Colorado, J. Geophys. Res. 99 (1994) 17997–18020.
[40] P. Robinson, R.J. Harrison, S.A. McEnroe, R.B. Hargraves, Lamellar magnetism in the hematite–ilmenite series as an explanation for strong remanent magnetization, Nature 418 (2002) 517–520.
[41] R.L. Wilson, Palaeomagnetism in Northern Ireland, Geophys. J. (Lond.) 5 (1961) 45–58.
[42] B. Efron, The Jackknife, The Bootstrap, and Other Resampling Plans, Society of Industrial and Applied Mathematics, Philadelphia, PA, 1982.
[43] C.M. Schlinger, D.R. Veblen, Magnetism and transmission electron microscopy of Fe–Ti oxides and pyroxenes in a granulite from Lofoten, Norway, J. Geophys. Res. 94 (1989) 14009–14026.
[44] G.E. Morgan, P.P.K. Smith, Transmission electron microscopy and rock–magnetic investigations of remanence carriers in a Precambrian metadolerite, Earth Planet. Sci. Lett. 53 (1981) 226–240.
[45] T.J. Armbrustmacher, N.G. Banks, Clouded plagioclase in metadolerite dikes, southeastern Bighorn Mountains, Wyoming, Am. Mineral. 59 (1974) 656–665.
[46] J. Bowles, J.S. Gee, D.V. Kent, M.R. Perfit, S.A. Soule, D.J. Fornari, Paleointensity applications to timing and extent of eruptive activity, 9°–10° N East Pacific Rise, Geochem. Geophys. Geosyst. 7 (2006) Q06006, doi:10.1029/2005GC001141.
[47] W. Zhou, R. Van der Voo, D.R. Peacor, Y. Zhang, Variable Ti-content and grain size of titanomagnetite as a function of cooling rate in very young MORB, Earth Planet. Sci. Lett. 179 (2000) 9–20.
[48] T. Pick, L. Tauxe, Characteristics of magnetite in submarine basaltic glass, Geophys. J. Int. 119 (1994) 116–128.
[49] P.P.K. Smith, Identification of single-domain titanomagnetite particles by means of transmission electron microscopy, Can. J. Earth Sci. 16 (1979) 375–379.
[50] D.M. Pechersky, K.S. Burakov, V.N. Vadkovskii, V.S. Zakharov, E.V. Sharkov, Z.V. Sharonova, Possibility of obtaining a record of the Early Proterozoic fine structure of the geomagnetic field: a preliminary analysis of results derived from petromagnetic and paleomagnetic study of the Monchegorsk Pluton, Izv. Phys. Solid Earth 38 (2002) 57–70.
[51] A. Yoshihara, Y. Hamano, Intensity of the Earth's magnetic field in late Archean obtained from diabase dikes of the Slave Province, Canada, Phys. Earth Planet. Int. 117 (2000) 295–307.
[52] M.W. McElhinny, M.E. Evans, An investigation into the strength of the geomagnetic field in the Early Precambrian, Phys. Earth Planet. Int. 1 (1968) 485–497.
[53] D.J. Dunlop, Y. Yu, Intensity and polarity of the field during Precambrian time, in: J.E.T. Channell, D.V. Kent, W. Lowrie, J.G. Meert (Eds.), Timescales of the Paleomagnetic Field, AGU Monograph 145, American Geophysical Union, Washington, D.C., 2004, pp. 85–100.
[54] R. Day, M. Fuller, V.A. Schmidt, Hysteresis properties of titanomagnetites: grain size and composition dependence, Phys. Earth Planet. Int. 13 (1977) 260–267.